Supplemental Data

Methods

Overexpression and purification of His-tagged *E. coli* proteins - All the proteins used in this study were purified as fusion proteins with a six-histidine tag. The cells harboring plasmids were grown at 37^{o}C in 2xYT media, with shaking at 220 rpm. When the cells density reached an $OD_{600}$of 0.5, 0.2 to 0.5 mM IPTG was added, the temperature was adjusted to 25^{o}C and cells left to overexpress proteins overnight. Cells were harvested by centrifugation at 4^{o}C and resuspended in 20mM Tris-HCl buffer, 500 mM NaCl, pH 7.5, 10% v/v glycerol. Cell paste was added with complete protease inhibitor (Roche) and DNase I (Sigma) before be put through a Constant Systems cell disrupter (1x10 Kpsi and 1x25 Kpsi, model Z-plus 1.1kW, Constant Systems) twice for cell lyses. Cell debris were removed by centrifugation at 13,000 x g (15 mins at 4^{o}C) and cell membranes were detained by ultracentrifugation at 125,000 x g (30 min at 4^{o}C) for membrane proteins, while the supernatant was collected for soluble proteins. Membranes pellets were then dissolved in 20mM Tris-HCl buffer, 100 mM NaCl, pH 7.5, 10% v/v glycerol, 5% v/v Triton X-100 or 1% w/v βDDM.

E. coli MacB purification - Membranes pellets were dissolved in 5% v/v Triton X-100 and MacB protein was purified under 0.2% v/v Triton X-100 by affinity chromatography using a Cu^{2+} charged HiTrap chelating column (GE Healthcare). After desalting, MacB samples were subjected to ion exchange chromatography, using a HiTrap Q column (GE Healthcare) and eluted using a NaCl gradient.

E. coli MacA and Δ20-MacA purification – MacA membrane pellets were dissolved in 5% v/v Triton X-100 and the MacA protein was purified under 0.2% v/v Triton X-100 by affinity chromatography using a HiTrap Ni^{2+} -chelating column and desalted afterwards. Δ20-MacA was purified as described for MacA but without the addition of detergent.

E. coli TolC purification – TolC was purified as described for the purification of MacA but with 1% w/v βDDM used to dissolve the membranes and 0.1% during the affinity-chromatography purification step.

Detergent exchange - MacB-TX-100 was mounted onto a HiTrap Q column and washed with 10 CV Tris HCl buffer, 10mM NaCl, 10% v/v glycerol, 0.2% w/v βDDM, pH 7.5 to remove TX-100 detergent. The column was then washed with an additional 2 CV with the same Tris-buffer containing 0.05% w/v βDDM. MacB-βDDM was then eluted from the column with 100mM NaCl in the same buffer. For analytical ultracentrifugation (AUC) experiments we further lowered the βDDM concentration to 0.006% w/v. Under these conditions MacB was stable for over a week, allowing several datasets to be collected from a single sample.

Quantification of βDDM bound to MacB - A colorimetric assay was applied to quantify βDDM contribution in MacB-βDDM complex [1]. MacB-βDDM complex and processing buffer, 20mM Tris HCl, 50mM NaCl, 10% glycerol, with or without 0.2% w/v βDDM, pH 7.5, were collected from after a detergent exchange process and the buffer with βDDM served as blank for correction of background in absorbance measurements. MacB-βDDM complex was diluted as necessary into the original purification buffer without βDDM to make a final volume of 60μL. The sample was fist mixed with 300μL phenol (5% w/v), then carefully added with 720 μL concentrated sulphuric acid and mixed well by vortexing with caps closed. The mixture was allowed to cool down at room temperature for 20 min and transferred to a cuvette for the absorbance measurements at 490nm using buffer with βDDM as a blank. A standard curve was generated using βDDM as a standard, and made by βDDM concentration (μg/60μL) plotting against the Abs_{490} using linear regression. The molar ratio of protein to detergent was then calculated. We determined the amount of detergent bound by MacB solubilized in 0.05% w/v

βDDM to be 1.2g βDDM/g MacB, which is equivalent to a βDDM:MacB molar ratio of 164: 1 and consistent with the values found for other membrane proteins [2]

Analytical ultracentrifugation data analysis - The buffer densities and partial specific volume of MacB were calculated with the program SEDNTERP [3] and using a partial specific volume of βDDM was 0.809 cm^3/g [4]. The equilibrium data was analyzed using SEDPHAT [5].

Atomic force microscopy - The molecular volumes of the protein particles were determined from particle dimensions based on AFM images. After adsorption of the receptors onto the mica support, the particles adopt the shape of a spherical cap. The heights and half-height radii were measured from multiple cross-sections of the same particle, and the molecular volume was calculated by using the following equation:

$$V_m = (\pi h/6)(3r^2 + h^2) \qquad (1)$$

where h is the particle height and r is the radius [6,7].

Molecular volume based on molecular mass was calculated by using the equation

$$V_c = (M_0/N_0)(V_1 + dV_2) \qquad (2)$$

where M_0 is the molecular mass, N_0 is Avogadro's number, V_1 and V_2 are the partial specific volumes of particle and water, respectively, and d is the extent of protein hydration [6,7]. We used the value of 0.74 cm^3/g for the partial specific volumes of protein [7], and 0.4 g of water per g of protein for the extent of protein hydration [8]. Using automated recognition of proteins [9, 10], it was calculated the molecular volume of isolated particles as described above.

ATPase activity - An EnzChek phosphate assay kit (Molecular Probes, Invitrogen) was used to determine the ATPase activity of MacB hydrolyzing ATP to release phosphate. The reaction mixture contained 20 mM Tris-HCl (pH 7.5), 50mM NaCl, 6mM $MgCl_2$, MESG substrate and purine nucleoside phosphorylase. The A_{360} absorbance change was measured, after initiating the reaction by mixing protein with ATP, using a stopped flow spectrometer (PiStar-180 spectrometer, Applied Photophysics) at 25^{o}C. A calibration curve, generated using KH_2PO_4 as a standard, was constructed by plotting the quantity of phosphate (nmoles) against the Abs_{360} of MESG. In control experiments in which the $MgCl_2$ was omitted, there was no ATPase activity.

The time course data for the production of inorganic phosphate (Pi) by MacB was analysed by fitting the trace, by non-linear regression, to an exponential function with a steady-state (e.g. Abs = $A_{(burst)}\exp(-k_b t) + k_{ss}t$), to give the rate ($k_b$) and amplitude ($A_{burst}$) of the Pi burst phase and steady-state rate (k_{ss}) of Pi production. In the presence of MacA, which prevented the Pi-burst by MacB, the traces were analysed by fitting the data to a linear function to give the steady-state rate of Pi production. The steady-state data for the rate of Pi release as a function of the ATP concentration was analysed by fitting the data points, by non-linear regression, to a hyperbolic function to yield values for V_{max} and K_m.

Equilibrium binding of [^{14}C]-erythromycin to affinity-purified Mac proteins – For equilibrium binding of erythromycin to purified Mac proteins, 50 µg of purified MacA or MacB, or 25 µg MacA plus 25 µg MacB were incubated for 30 min in the presence of fixed concentrations of 1, 5 or 10 µM [N-methyl-^{14}C]-erythromycin (48.8 mCi/mmol, Perkin Elmer Life sciences, USA). The incubation was carried out in glass tubes in a final volume of 500 µl of 10 mM Tris–HCl (pH 7.4) containing 0.05% w/v DDM. The samples were incubated at room temperature in the dark, and rapidly filtered through 0.22 µM nitrocellulose filters (Whatmann), which were pre-equilibrated for 5 h in wash buffer (ice-cold 10 mM Tris–HCl (pH 7.4) supplemented with 150 mM KCl and 5 mM

$MgCl_2$). The filters were washed once with 3 ml of wash buffer. Subsequently, filter-retained radioactivity was measured by liquid scintillation counting using the scintillant Ultima Gold XR (Perkin Elmer Life Sciences, USA). Non-specific binding to MacB (less than 30% of total binding) was determined as the amount of [^{14}C]-erythromycin bound to half molar quantities of 12 trans-membrane helix-containing sugar transporter GalP [11,12], and was subtracted.

Supplemental Figure Legends

Fig. 1 - MacA sequence alignment. A sequence alignment of the MacA membrane fusion proteins from the Gram-negative bacterium *E. coli* and Gram-positive bacteria *S. epidermitis* and *S.aureus* respectively This analysis indicates that while the proteins from *E. coli* and *S. epidermitis* have similar secondary structures, the large α-helical domain predicted to harbor the TolC interaction site is missing in the *S. aureus* protein. Alignments were performed using T-Coffee and ClustalW2 server. Secondary structure prediction is a summary of PHD, PROFsec and JPred secondary structure predictions with probability weighting as implicated in PredictProtein/MetaPP server [13]. Results were visualized using ESPript [14].

Fig. 2 – (A) Chemical cross-linking indicates that MacA interacts with MacB. The chemical cross-linker DMS (dimethyl-suberimidate; 11.0 Å spacer arm) was added to MacA, MacB, and a mixture of the two proteins, and the cross-linked products analysed by SDS-PAGE. The lanes of the gel were loaded with the following samples: MacA + 5mM DMS (lane 1); MacB + 5mM DMS (lane 2); MacB + MacA +5mM DMS 1 h (lane 3); MacB+ 5 mM DMS 30 min + MacA (another 30 min) (lane 4). A novel band, shown within a box, was identified, which was subsequently found to contain both by MacA and MacB when analysed by MALDI-TOF in-gel analysis. The right hand panels show the MacB and MacA sequences and oligopeptides identified by MALDI-TOF mass spectrometry are indicated in red. In control lanes only MacB or MacA could be identified by MALDI in-gel analyses (data not shown). **(B) Chemical cross-linking indicates that MacB forms dimers.** The MacB protein

was mixed with increasing concentrations of the chemical cross-linker DSP (dithiobis(succinimidyl)-propionate; 12.0 Å spacer arm) and the cross-linked products analysed by SDS-PAGE. In addition to the band corresponding to the monomer, with a Mr between 60-70 kDa, the most predominant band, which increased in intensity with the DMS concentration, ran between the 120 kDa and 160 kDa markers, indicative of a dimer. However, there were several higher-Mr bands also present that would suggest that the protein can form higher-order oligomers.

References

1. Butler PJ, Ubarretxena-Belandia I, Warne T, Tate CG (2004) The *Escherichia coli* multidrug transporter EmrE is a dimer in the detergent-solubilised state. J Mol Biol. 340:797-808
2. Ravaud S, Do Cao MA, Jidenko M, Ebel C, Le Maire M, Jault JM, Di Pietro A, Haser R, Aghajari N. (2006) The ABC transporter BmrA from *Bacillus subtilis* is a functional dimer when in a detergent-solubilized state. Biochem J. 395:345-53
3. Laue TM, Shah BD, Ridgeway TM, Pelletier SL. Computer-aided interpretation of analytical sedimentation data for proteins in: Analytical ultracentrifugation in Biochemistry and polymer science (Harding, S.E., Rowe, A. J. and Horton eds) pp 90-125, The Royal Society of Chemistry, Cambridge, UK.
4. Peterson GL, Rosenbaum LC, Schimerlik MI. Solubilization and hydrodynamic properties of pig atrial muscarinic acetylcholine receptor in dodecyl β-D-maltoside. Biochem J. (1988) 255: 553-60
5. Vistica J, Dam J, Balbo A, Yikilmaz E, Mariuzza RA, Rouault TA, Schuck P. (2004) Sedimentation equilibrium analysis of protein interactions with global implicit mass conservation constraints and systematic noise decomposition. Analytical Biochemistry 326: 234-256

6. Barrera NP, Herbert P, Henderson RM, Martin IL, Edwardson JM. (2005) Atomic force microscopy reveals the stoichiometry and subunit arrangement of 5-HT3 receptors. Proc Natl Acad Sci U S A. 102: 12595-12600.

7. Schneider SW, Lärmer J, Henderson RM, Oberleithner H. (1998) Molecular weights of individual proteins correlate with molecular volumes measured by atomic force microscopy. Pflugers Arch. 435: 362-367.

8. Grant EH. (1957) The dielectric method of estimating protein hydration Phys Med Biol. 2: 17-28.

9. Barrera NP, Henderson RM, Edwardson JM. (2008) Determination of the architecture of ionotropic receptors using AFM imaging. Pflugers Arch. 456:199-209

10. Barrera NP, Ge H, Henderson RM, Fitzgerald WJ, Edwardson JM. (2008). Automated analysis of the architecture of receptors, imaged by atomic force microscopy. Micron *39*, 101-110.

11. Bapna A, Federici L, Venter H, Velamakanni S, Luisi B, Fan TP, van Veen HW. (2007) Two proton translocation pathways in a secondary active multidrug transporter. J. Mol. Microbiol. Biotechnol. 12:197-209

12. Velamakanni S, Janvilisri T, Shahi S, van Veen HW. (2008) A functional steroid-binding element in an ATP-binding cassette multidrug transporter. Mol Pharmacol. 73: 12-17.

13. Rost B, Yachdav G, Liu J. (2004) The PredictProtein Server. Nucleic Acids Research 32(Web Server issue):W321-W326.

14. Gouet P, Courcelle E, Stuart DI, Metoz F. (1999) ESPript: multiple sequence alignments in PostScript. Bioinformatics. 15:305-8

15. Miroux B, Walker J. (1996) Over-production of proteins in *Escherichia coli* mutant hosts that allow synthesis of some membrane proteins and globular proteins. J. Mol Biol. 260:289-98

16. Morita Y, Kodama K, Shiota S, Mine T, Kataoka A, Mizushima T, Tsuchiya T. (1998) NorM, a putative multidrug efflux protein, of *Vibrio parahaemolyticus* and its homolog in *Escherichia coli*. Antimicrob Agents Chemother. 42:1778-82

TABLE 1: Strains and plasmids

Strains/plasmids	*Description*	*Source*
***E. coli* strains**		
NovaBlue	Source of DNA for PCR amplification of *macAB* and *tolC* genes – *recA1 endA1 gyrA96 thi-1 hsdR17 supE44 relA1 lac* [F' *proAB lacI*^{q}*ZΔM15 Tn10*(Tet^{r})]	Novagen
C43(DE3)	Expression host for pET vectors - F- *ompT hsdS*$_B$ (r_B-m_B-) *gal dcm* (DE3)	15
Kam3(DE3)	Antibiotic sensitive host strain used for expression of pDuet vectors - Δ*acrAB*	16
Plasmid cloning vectors		
pET21	Expression of His-tagged proteins in *E. coli*	Novagen
pET28	Expression of His-tagged proteins in *E. coli*	Novagen
pET45	Expression of S-tagged proteins in *E. coli*	Novagen
pET-Duet	Simultaneous expression of two proteins in *E. coli*	Novagen
pBAD/gIII	Expression of His-tagged proteins that are secreted into the periplasm of *E. coli*	Invitrogen
Plasmid constructs		
pET-macB	*E.coli macB* cloned into pET28a(+) using NdeI-macB Forward and SacI-stop-macB Reverse primers	This study
pET-macA	*E. coli macA* cloned into pET21d(+) using NcoI-macA Forward and XhoI-macA Reverse primers	This study
pET-Δ20macA	*E. coli macA* mutant, encoding a derivative truncated at position 20, cloned into pET21d(+) using NcoI-FD20-macA Forward and XhoI-macA Reverse primers	This study
pET-tolC	*E. coli tolC* double mutant, Y362F,R367D, encoding residues 1-450 of TolC in the open-state, cloned into pET21a(+) using NdeI-tolC Forward and XhoI-RD43tolC Reverse primers	This study
pET-Duet-macB	*E. coli macB* cloned into MCS1 of pET-Duet, using EcoRI-macB Forward and Sal1-stop-macB Reverse primers.	This study
pET-Duet-macB/macA	*E. coli macBmacA* cloned into MCS1 of pET-Duet using using EcoRI-macB Forward, Sal1-stop-macB Reverse, and Sal1-SD-macA Forward, Not1-stop-T7tag-macA Reverse primer, respectively.	This study
pET-Duet-macB/tolC	*E. coli macB* and *tolC* cloned into MCS1 and MCS2 of pET-Duet, using EcoRI-macB Forward, Sal1-stop-macB Reverse, and NdeI-tolC Forward, XhoI-RD43tolC Reverse primers, respectively.	This study
pET-Duet-macB/macA/tolC	*E. coli macBmacA* cloned into MCS1 and *tolC* into MCS2 of pET-Duet for drug susceptibility testing, using EcoRI-macB Forward, Sal1-stop-macB Reverse, Sal1-SD-macA Forward, Not1-stop-T7tag-macA Reverse, and NdeI-tolC Forward, XhoI-RD43tolC Reverse primers, respectively.	This study
pET-Duet-macB/gIII-SS-Δ20macA/tolC	*E. coli macB* and *Δ20macA*, bearing an N-terminal gIII signaling sequence, cloned into MCS1 and *tolC* into MCS2 of pET-Duet for drug susceptibility testing. This was achieved by ligating a NcoI-*Δ20macA*-XhoI fragment into pBAD/gIII; a SalI-geneIII SS-*Δ20MacA*-T7tag-stop-NotI fragment was then raised with SalI-SD-gIII Seqence Forward, Not1-stop-T7tag-macA Reverse and ligated into pET Duet.	This study
pET-macA (S-tag)	*E. coli macA* cloned into pET45b(+) using NcoI-macA Forward and XhoI-macA Reverse primers	This study
pET-tolC (S-tag)	*E. coli tolC* cloned into pET45b(+) using NcoI-tolC Forward and XhoI-RD43tolC *R*everse primers	This study

TABLE 2: Primers

Primers	
NdeI-macB Forward	**CAT ATG** ACG CCT TTG CTC GAA TTA AAG GAT
SacI-stop-macB Reverse	**GAG CTC** TCA CTC TCG TGC CAG AGC ATC TAC
NcoI-macA Forward	**CCA TGG** GA GCA TAT GGA GTA TTC AGA AAA TTT
XhoI-macA Reverse	**CTC GAG** TTG TGC AGC TCC TGG TTT GGC CTC
NcoI-FD20-macA Forward	**CCA TGG** GA GGA CTG ATT ACG TTA TGG AGA ATT
XhoI-macA Reverse	**CTC GAG** TTG TGC AGC TCC TGG TTT GGC CTC
NdeI-tolC Forward	**CAT ATG** AAG AAA TTG CTC CCC ATT CTT ATC
NcoI-tolC Forward	**CCA TGG** GA AAG AAA TTG CTC CCC ATT CTT ATC
XhoI-RD43tolC Reverse	**CTC GAG** TTC CGG ATT AGT GGA AAC CGG TTT
EcoRI-macB Forward	**GAA TTC** G ACG CCT TTG CTC GAA TTA AAG GAT
Sal1-stop-macB Reverse	**GTC GAC** TCA CTC TCG TGC CAG AGC ATC TAC
Sal1-SD-macA Forward	**GTC GAC** GAG GAA TAA TAA ATG GCA TAT GGA GTA TTC AGA AAA
Not1-stop-T7tag-macA Reverse	**GCGG CCGC** TCA ACC CAT TTG CTG TCC ACC AGT CAT GCT AGC CAT TTG TGC AGC TCC TGG TTT GGC CTC ACC AAT CAC CAC TTC ATC GC
NdeI-tolC Forward	**CAT ATG** AAG AAA TTG CTC CCC ATT CTT ATC
XhoI-RD43tolC Reverse	**CTC GAG** TTC CGG ATT AGT GGA AAC CGG TTT
SalI-SD-gIII Seqence Forward	**GTC GAC** GAG GAA TAA TAA ATG AAA AAA CTG CTG TTC GCG ATT
Not1-stop-T7tag-macA Reverse	**GCGG CCGC** TCA ACC CAT TTG CTG TCC ACC AGT CAT GCT AGC CAT TTG TGC AGC TCC TGG TTT GGC CTC ACC AAT CAC CAC TTC ATC GC

Notes: **Bolded** sequences indicate restriction endonuclease sites. Underlined sequences indicate stop codons incorporated to prevent addition of vector sequences into the transcription.

Supplementary Figure 1.

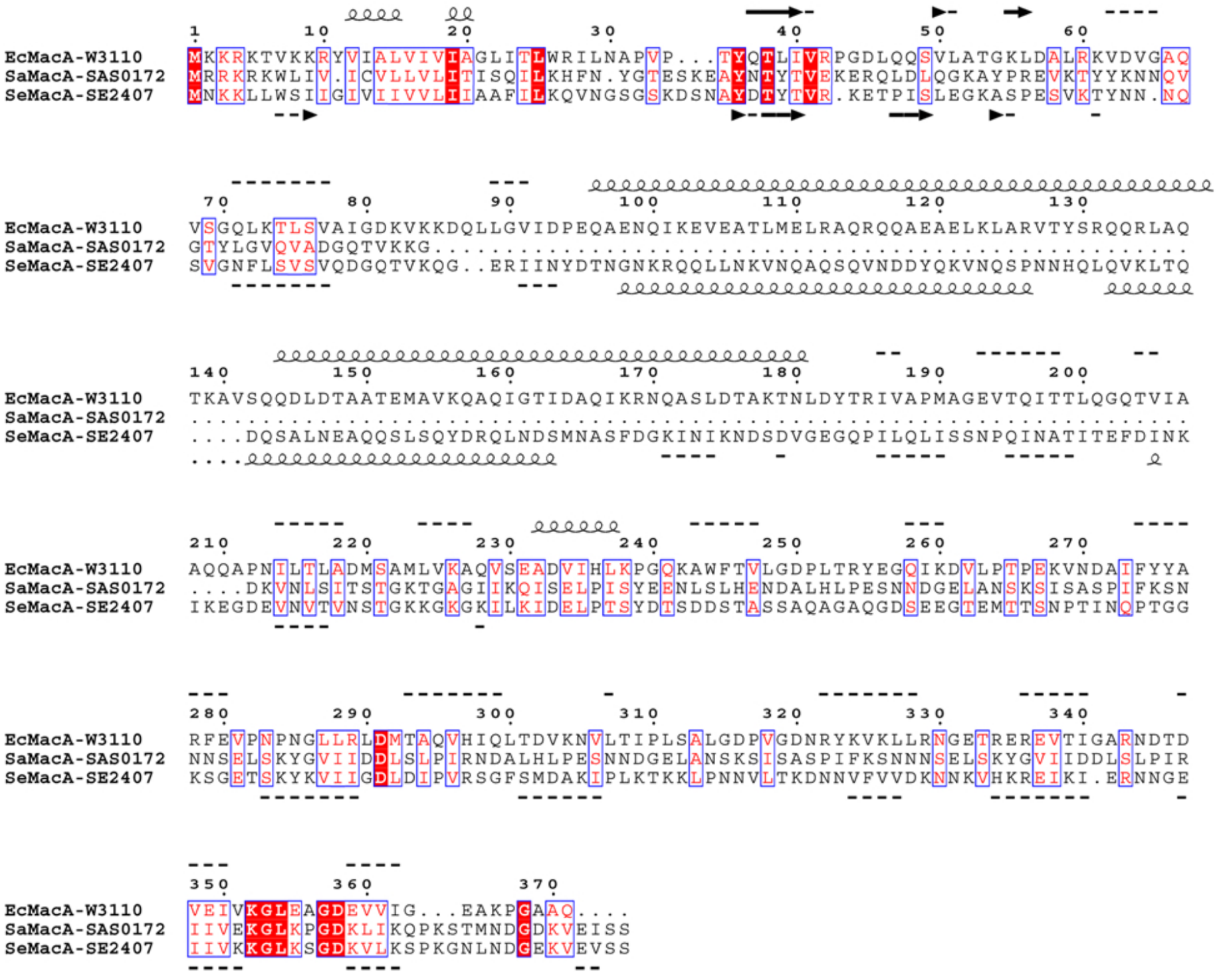

Supplementary Figure 2.

A

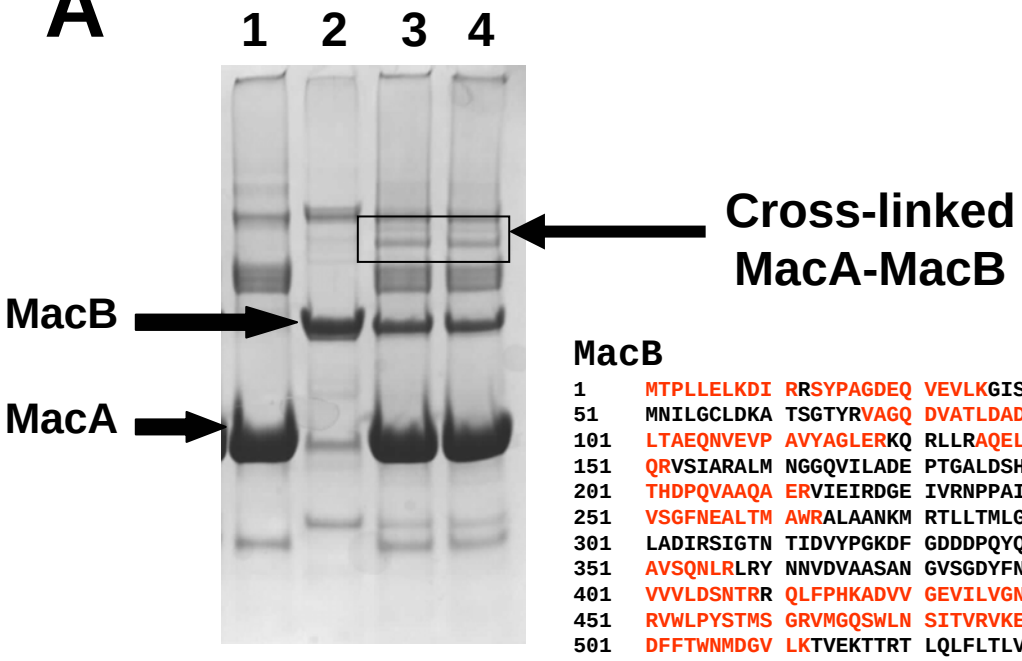

MacB

```
1     MTPLLELKDI RRSYPAGDEQ VEVLKGISLD IYAGEMVAIV GASGSGKSTL
51    MNILGCLDKA TSGTYRVAGQ DVATLDADAL AQLRREHFGF IFQRYHLLSH
101   LTAEQNVEVP AVYAGLERKQ RLLRAQELLQ RLGLEDRTEY YPAQLSGGQQ
151   QRVSIARALM NGGQVILADE PTGALDSHSG EEVMAILHQL RDRGHTVIIV
201   THDPQVAAQA ERVIEIRDGE IVRNPPAIEK VNVTGGTEPV VNTVSGWRQF
251   VSGFNEALTM AWRALAANKM RTLLTMLGII IGIASVVSIV VVGDAAKQMV
301   LADIRSIGTN TIDVYPGKDF GDDDPQYQQA LKYDDLIAIQ KQPWVASATP
351   AVSQNLRLRY NNVDVAASAN GVSGDYFNVY GMTFSEGNTF NQEQLNGRAQ
401   VVVLDSNTRR QLFPHKADVV GEVILVGNMP ARVIGVAEEK QSMFGSSKVL
451   RVWLPYSTMS GRVMGQSWLN SITVRVKEGF DSAEAEQQLT RLLSLRHGKK
501   DFFTWNMDGV LKTVEKTTRT LQLFLTLVAV ISLVVGGIGV MNIMLVSVTE
551   RTREIGIRMA VGARASDVLQ QFLIEAVLVC LVGGALGITL SLLIAFTLQL
601   FLPGWEIGFS PLALLLAFLC STVTGILFGW LPARNAARLD PVDALARE
```

MacA

```
1     MKKRKTVKKR YVIALVIVIA GLITLWRILN APVPTYQTLI VRPGDLQQSV
51    LATGKLDALR KVDVGAQVSG QLKTLSVAIG DKVKKDQLLG VIDPEQAENQ
101   IKEVEATLME LRAQRQQAEA ELKLARVTYS RQQRLAQTKA VSQQDLDTAA
151   TEMAVKQAQI GTIDAQIKRN QASLDTAKTN LDYTRIVAPM AGEVTQITTL
201   QGQTVIAAQQ APNILTLADM SAMLVKAQVS EADVIHLKPG QKAWFTVLGD
251   PLTRYEGQIK DVLPTPEKVN DAIFYYARFE VPNPNGLLRL DMTAQVHIQL
301   TDVKNVLTIP LSALGDPVGD NRYKVKLLRN GETREREVTI GARNDTDVEI
351   VKGLEAGDEV VIGEAKPGAA Q
```

B